

Neutron Rietveld analysis for optimized $\text{CaMgSi}_2\text{O}_6:\text{Eu}^{2+}$ and its luminescent properties

Won Bin Im

Department of Materials Science and Engineering, Korea Advanced Institute of Science and Technology, Daejeon 305-701, Republic of Korea

Yong-Il Kim

Korea Research Institute of Standards and Science, Yuseong, Daejeon 305-600, Republic of Korea

Jong Hyuk Kang and Duk Young Jeon^{a)}

Department of Materials Science and Engineering, Korea Advanced Institute of Science and Technology, Daejeon 305-701, Republic of Korea

Ha Kyun Jung and Kyeong Youl Jung

Advanced Materials Division, Korea Research Institute of Chemical Technology, Yuseong-gu, Daejeon 305-600, Republic of Korea

(Received 15 February 2005; accepted 7 April 2005)

We optimized synthesis conditions of blue-emitting $\text{CaMgSi}_2\text{O}_6:\text{Eu}^{2+}$ (CMS:Eu²⁺) with conventional solid-state reaction and successfully determined structure parameters by Rietveld refinement method with neutron powder diffraction data. The final weighted R -factor R_{wp} was 6.42% and the goodness-of-fit indicator $S (= R_{\text{wp}}/R_e)$ was 1.34. The refined lattice parameters of CMS:Eu²⁺ were $a = 9.7472(3) \text{ \AA}$, $b = 8.9394(2) \text{ \AA}$, and $c = 5.2484(1) \text{ \AA}$. The β angle was $105.87(1)^\circ$. The concentration quenching process was observed, and the critical quenching concentration of Eu²⁺ in CMS:Eu²⁺ was about 0.01 mol and critical transfer distance was calculated as 12 \AA . With the help of the Rietveld refinement and Dexter theory, the critical transfer distance was also calculated as 27 \AA . In addition, the dominant multipolar interaction of CMS:Eu²⁺ was investigated from the relationship between the emission intensity per activator concentration and activator concentration. The dipole–dipole interaction was a dominant energy transfer mechanism of electric multipolar character of CMS:Eu²⁺.

I. INTRODUCTION

$\text{BaMgAl}_{10}\text{O}_{17}:\text{Eu}^{2+}$ (BAM) is an efficiency blue phosphor for plasma display panels (PDPs) because of its high luminescence under vacuum ultraviolet (VUV) excitation. However, the luminance decrease and color shift of this phosphor that occur during the baking process are well known problems. The thermal degradation of the phosphor that occur during the baking process is a particularly serious problem for manufacturing of PDP panels. It has been reported that the thermal degradation of BAM is probably related to the change of either the valence of Eu²⁺ to Eu³⁺ or its crystal structure (β -alumina), which has an open layer in the crystal.^{1–3}

Based on this information, $\text{CaMgSi}_2\text{O}_6:\text{Eu}^{2+}$ (CMS:Eu²⁺) has been proposed as a way to overcome the drawbacks of BAM because it is more stable under the baking process and has relatively good photoluminescence (PL)

properties under VUV excitation.^{2,3} However, the PL intensity of CMS:Eu²⁺ excited by 147 nm sources is weaker than that of BAM, and the study on crystal structure of CMS:Eu²⁺ also has not been done sufficiently. To obtain CMS:Eu²⁺ phosphor of high luminescence efficiency, we have optimized it in terms of factors such as activator concentration, gas flow rates, and SiO₂ ratios. Since, in 147 nm excitation, the excitation wavelength is shorter than absorption edge of the host lattice, the VUV spectrum does not excite an activator directly. In addition, the VUV spectrum is very well absorbed into the CMS crystal so its penetration depth into the phosphor particle is very small. For this reason, CMS:Eu²⁺ phosphor must have a property of high energy transfer from host lattice to activators.¹

Furthermore, the precise crystal structural information of CMS:Eu²⁺ is necessary to improve its optical property. In addition to this, it is highly desirable to initiate a detailed electronic structure study. The blue emission band of CMS:Eu²⁺ is mainly caused by the Eu²⁺ luminescent center, which may have replaced Ca²⁺ sites

^{a)}Address all correspondence to this author.

e-mail: dyj@kaist.ac.kr

DOI: 10.1557/JMR.2005.0253

partially in the CMS compound. In particular, it is very important to determine the quantitative amount of Eu²⁺ in the crystal lattice because the amount of Eu²⁺ doped into the crystal lattice is directly related to optical properties of CMS:Eu²⁺; thus an accurate description of the location and population degree of Eu²⁺ ions in CMS:Eu²⁺ is essential.

In this study, we optimized blue-emitting CMS:Eu²⁺ and performed the crystal structural refinement of CMS:Eu²⁺ by means of Rietveld refinement using neutron powder diffraction data. In addition, we investigated the mechanism of energy transfer in Eu²⁺ of critical concentration and Dexter's theory for energy transfer.

II. EXPERIMENTAL

Powder samples of CMS:Eu²⁺ were prepared by conventional solid-state reaction. To synthesize CMS:Eu²⁺ phosphor, CaCO₃ (Kojundo, Japan, 99.99%), MgO (Aldrich 99.99%), SiO₂ (Kojundo, Japan, 99.99%), and EuF₃ (Aldrich 99.99 %) were used as raw materials. Small quantities of NH₄F were added as a flux. The raw materials were mixed in a ball mill mixer for 12 h and heated subsequently at 1150 and 1200 °C in a reducing atmosphere of H₂ (5%) and N₂ (95%) for 3 h, respectively. PL spectra were obtained at room temperature by scanning wavelength region from 350 to 600 nm under an excitation of 147 nm radiation from a deuterium lamp. The excitation spectrum in VUV region was corrected by sodium salicylate.

Neutron powder diffraction data were collected over scattering angles ranging from 0° to 160° using 1.8348 Å neutron on high resolution powder diffractometer (HRPD) at the Hanaro Center of the Korea Atomic Energy Research Institute in Daejeon, Korea. The General Structure Analysis System (GSAS) program was used to do the structural refinement.⁴ A pseudo-Voigt function was chosen as the best trial profile function among many possible profile functions in GSAS.⁷ The neutron scattering lengths for Ca, Mg, Si, and O atoms are 0.4700, 0.5375, 0.4149, and 0.5803 × 10⁻¹² cm, respectively.

III. RESULTS AND DISCUSSION

A. Optimization of Ca_{0.99}MgSi_{2.2}O₆:0.01Eu²⁺ phosphor for high luminance

The dependence of emission intensity on Eu concentration is presented in Fig. 1. We investigated the PL intensity of the CMS:Eu²⁺ with varying Eu concentrations from 0.005 to 0.3 mol. It was found that the optimum concentration of Eu for CMS:Eu²⁺ was 0.01 mol. From more than 0.1 mol of activator concentration, a significant drop in relative emission intensity was observed, due to concentration quenching.

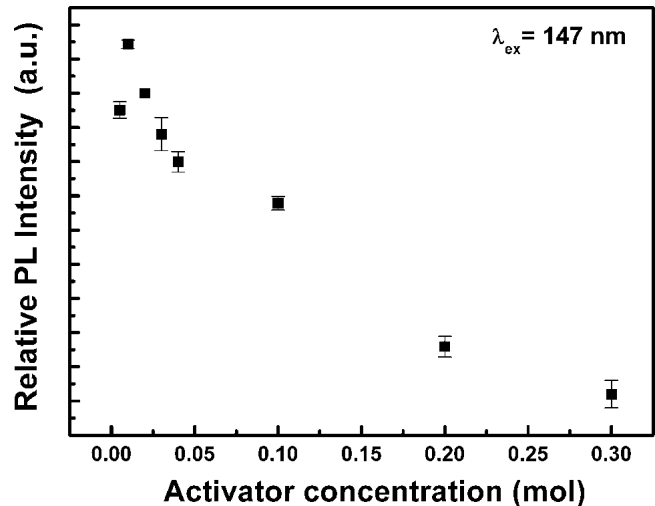


FIG. 1. VUV/PL intensities of CMS:Eu²⁺ phosphor prepared with varying activator concentration.

Figure 2 shows the relative PL intensity of CMS:Eu²⁺ phosphors as a function of gas flow rates with the concentration of activator Eu fixed at 0.01 mol. As shown in Fig. 2, the gas flow rate was optimized at 0.2 l/min. In this case, the body color of the phosphor powders appears white. As gas flow rate increases over 0.2 l/min, the crystallinity of the host material became poor due to strong reducing atmosphere. In addition, light yellow color phosphor powders were obtained when gas flow rate was more than 0.6 l/min because the host lattice was reduced strongly. In contrast, when weak reducing atmosphere was introduced, the Eu³⁺ ions was not easily reduced to Eu²⁺ ions. It was found from these results that the PL intensity of CMS:Eu²⁺ was very easily affected by synthesis conditions.

We also performed experiments with varying SiO₂ mole ratios to improve the PL intensity of CMS:Eu²⁺

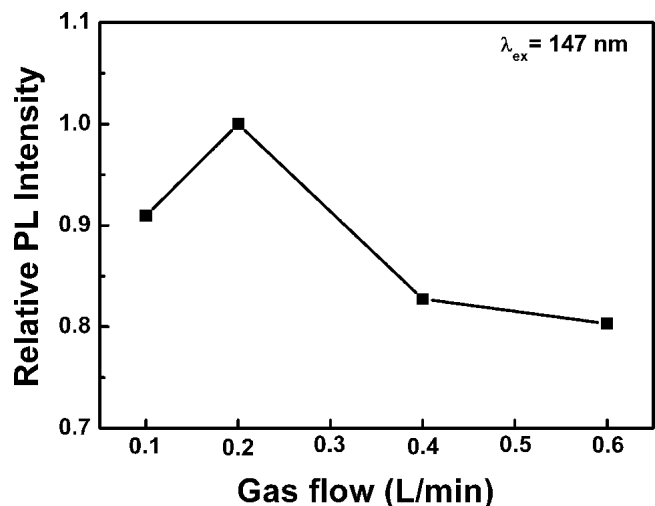


FIG. 2. Relative PL intensities depending upon gas flow rates.

phosphor. According to Ropp's report,⁵ a small amount of excess SiO_2 is used in synthesis of inorganic phosphor materials to ensure a complete solid-state reaction among the reacting species and to avoid the presence of strongly absorbing cationic species in the final product. However, if the amount of SiO_2 is beyond a critical value, the PL intensity may decrease considerably due to the increase of unreacted SiO_2 per unit area. For this reason, it is essential to quantitatively determine the quantity of SiO_2 phase in inorganic phosphors. Figure 3 shows relative PL intensity depending upon SiO_2 mol ratios. The stoichiometric ratio of $\text{CaO}:\text{MgO}:\text{SiO}_2$ is 1:1:2 for $\text{CMS}:\text{Eu}^{2+}$. However, the highest brightness can be obtained when 0.2 mol excess SiO_2 is introduced in the starting mixture of raw materials. For the 0.2 mol excess SiO_2 , PL intensity increased by about 10% in comparison with that of stoichiometric composition. It is well known that in the case of $\text{Zn}_2\text{SiO}_4:\text{Mn}^{2+}$, the highest brightness can be obtained with excess SiO_2 .⁶ Above 0.2 mol excess SiO_2 , PL intensity decreased as much as 25% due to increase of unreacted SiO_2 per unit area.

B. Structural refinement of optimized $\text{Ca}_{0.99}\text{MgSi}_{2.2}\text{O}_6:0.01\text{Eu}^{2+}$ phosphor

The structural refinement was carried out for the optimized $\text{CMS}:\text{Eu}^{2+}$ phosphor. A reasonable approximation of the actual crystal structure as a starting model is required to do the crystal structural refinement. The starting structural model for $\text{CMS}:\text{Eu}^{2+}$ was built with the crystallographic data reported by Levien et al.⁸ This was based on the $C12/c1$ space group.

Although the convergence was achieved by the initial structural refinement, some unknown diffraction peaks remained unaccounted for within the experimental profile. Considering the starting materials and experimental variables such as pressure, temperature, and environment

atmosphere, CaO , SiO_2 , MgO , EuO , CaSiO_3 , etc., might be proposed to exist within $\text{CMS}:\text{Eu}^{2+}$ samples. Of these possible phases, the remaining reflection peaks could be indexed satisfactorily to SiO_2 (cristobalite). Consequently, the synthesized sample was composed of $\text{CMS}:\text{Eu}^{2+}$ and SiO_2 phases. The initial structure model of SiO_2 as a secondary phase was based on the crystallographic data of SiO_2 with the space group $P4_12_1$.⁹

The disorder of Eu^{2+} ions was considered after refinement with two-phase model for the synthesized sample. When Eu^{2+} ions are incorporated into the crystal structure of CMS , Eu^{2+} ions may substitute for all cationic sites, Ca^{2+} , Mg^{2+} , and Si^{4+} . However, considering their respective ionic radii and allowed oxygen-coordination number (n)— Mg^{2+} (0.72 Å, $n = 6$), Si^{4+} (0.26 Å, $n = 4$), Ca^{2+} (1.12 Å, $n = 8$) and Eu^{2+} (1.25 Å, $n = 8$)¹⁰—it is difficult for Eu^{2+} ions to substitute for Mg^{2+} or Si^{4+} ions.⁵ Therefore, the structural refinement proceeded under the assumption that Eu^{2+} ions substituted for only Ca^{2+} ions. Consequently, the Rietveld refinement was carried out under the assumption that Eu^{2+} ions substituted only for Ca^{2+} ions. The occupancies of Eu^{2+} and Ca^{2+} sites were constrained so that both sites were fully occupied, and the total occupancy of Eu^{2+} and Ca^{2+} ions was maintained to be unity. The temperature factors of the atoms to occupy the two sites were set to be equal. Through the preliminary structural refinement, the background, scale factor, lattice parameters, profile parameters, asymmetrical parameters, atomic positions, and isotropic atomic displacements, etc., for all atoms, were optimized. After this structural refinement had converged, the occupation factors were refined with the constraints of occupation and thermal factors.

Figure 4 shows the structural refinement patterns for the mixture model of $\text{CMS}:\text{Eu}^{2+}$ and SiO_2 phases. The final weighted R -factor R_{wp} was 6.42 %, and the goodness-of-fit indicator $S (= R_{\text{wp}}/R_e)$ was 1.34. Table I listed the refined structural parameters of $\text{CMS}:\text{Eu}^{2+}$ obtained from the above structural refinement. The occupations of Eu atoms occupying the Ca sites are 0.013 and totally substitute for 1.3% of the Ca atoms. The weight fractions of $\text{CMS}:\text{Eu}^{2+}$ and SiO_2 based on the scale factors were 96.45(2)% and 3.55(2)%, respectively. The refined lattice parameters of $\text{CMS}:\text{Eu}^{2+}$ were $a = 9.7472(3)$, $b = 8.9394(2)$ Å, and $c = 5.2484(1)$ Å. The β angle was $105.87(1)^\circ$.

C. Photoluminescence properties of $\text{Ca}_{0.99}\text{MgSi}_{2.2}\text{O}_6:0.01\text{Eu}^{2+}$ phosphor

Figure 5 shows the excitation and PL spectra of the optimized $\text{CMS}:\text{Eu}^{2+}$ under a 147 nm excitation. In the excitation spectrum, direct excitation bands appeared from 250 to 320 nm. Its emission was measured at 447 nm. The emission band corresponds to the transition from the $4f^65d$ excited state to the $4f^7$ ground state of a

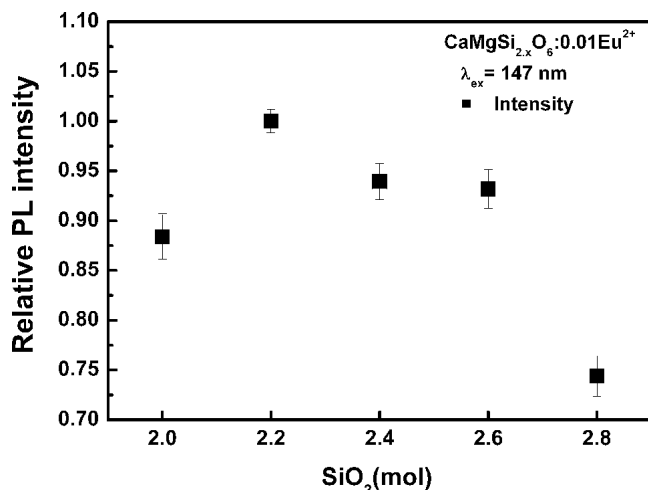


FIG. 3. VUV/PL intensities of $\text{CMS}:\text{Eu}^{2+}$ phosphor prepared with varying SiO_2 ratio.

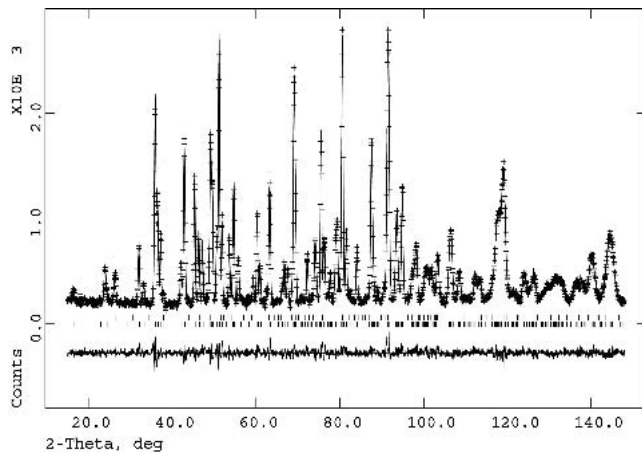


FIG. 4. Structural refinement patterns of a mixture CMS:Eu²⁺ and SiO₂ phases using neutron powder diffraction data. Plus (+) marks represent the observed intensities, and the solid line defines calculated ones. A difference (observed – calculated) plot is shown beneath. Tick marks above the difference indicate the reflection positions. The upper and lower tick marks indicate the reflection positions for SiO₂ and CMS:Eu²⁺ phases, respectively.

Eu²⁺ ion.¹¹ The obtained CIE color coordinates of the synthesized CMS:Eu²⁺ were $x = 0.148$, $y = 0.0389$.

To understand the energy transfer mechanism of CMS:Eu²⁺, it is useful to know the critical distance (R_c) for energy transfer between the sensitizer and activator. In this study, we used Dexter's formula,¹² which represents restricted transfer of electric dipole–dipole interaction since we are dealing with allowed electric–dipole

transitions in the case of Eu²⁺. The probability of transfer dipole–dipole interaction has been given by Dexter as

$$R_c^6 = 0.63 \times 10^{28} \frac{4.8 \times 10^{-16} \cdot P}{E^4} \text{SO} \quad (1)$$

Here P is the oscillator strength of the Eu²⁺ ion, E is the energy of maximum spectral overlap, and SO is the spectral overlap integral,¹³ which represents the product of normalized spectral shapes of emission and excitation. The values of E and SO can be derived from the spectral data in Fig. 5. For P corresponding to the broad $4f^7 \rightarrow 4f^65d$ absorption band, a value of 10^{-2} is taken.^{13,14} The values of E and SO are obtained from the spectra, which are 2.97 eV and $1.1 \times 10^{-2} \text{ eV}^{-1}$ ($0.5 \times \text{height} \times \text{width} = 0.5 \times 0.12 \times 0.19$), respectively. From Eq. (1), the value of R_c for the energy transfer in CMS:Eu²⁺ was calculated as 12 Å.

In addition, it is possible to calculate the R_c from the data of concentration quenching and number of cations present in the unit cell. In this case, the critical distance is equal to the average shortest distance between the nearest activator ions corresponding to the critical concentration (X_c).¹⁵ The critical distance from data concentration quenching is represented as

$$R_c \approx 2 \left(\frac{3V}{4\pi X_c N} \right)^{1/3} \quad (2)$$

TABLE I. Structural parameters of CMS:Eu²⁺ obtained from the structural refinement using neutron powder diffraction data taken at room temperature. The symbols, g and U_{iso} , represent the occupation factor and isotropic thermal parameter, respectively. The numbers in parentheses are the estimated standard deviations of the last significant figure.

Atom	Site	x	y	z	g	$100 U_{\text{iso}}/\text{Å}^2$
CaMgSi ₂ O ₆ :Eu ²⁺						
Ca	4e	0.0	0.3003(2)	0.25	0.987(1) ^a	1.69(3) ^b
Eu	4e	0.0	0.3003(2)	0.25	0.013(1)	1.69(3)
Mg	4e	0.0	0.9087(2)	0.25	1.0	0.68(2)
Si	8f	0.2858(2)	0.0934(2)	0.2283(3)	1.0	0.45(2)
O	8f	0.1158(1)	0.0868(2)	0.1415(2)	1.0	0.78(3)
O	8f	0.3619(2)	0.2490(3)	0.3182(3)	1.0	1.05(2)
O	8	0.3508(3)	0.0171(2)	0.9932(3)	1.0	0.71(3)
Space group: $C12/c1$ (No. 15) and $Z = 4$ $a = 9.7472(3)$, $b = 8.9394(2)$ Å and $c = 5.2484(1)$ Å; $\beta = 105.87(1)^\circ$						
SiO ₂						
Si	4a	0.2191(23) ^b	0.2191(23)	0.0	1.0	2.86(31)
O	8b	0.2389(32)	0.0841(24)	0.2000(37)	1.0	2.84(42)
Space group: $P4_12_12$ (No. 92) and $Z = 2$ $a = b = 4.9882(22)$ Å and $c = 6.937(59)$ Å						
Weight fraction		CaMgSi ₂ O ₆ :Eu ²⁺		SiO ₂		
		96.45(2)%		3.55(2)%		

^aConstraint on occupancy: $g(\text{Ca}) + g(\text{Eu}) = 1.0$.

^bConstraint on isotropic thermal factor: $U_{\text{iso}}(\text{Ca}) = U_{\text{iso}}(\text{Eu})$.

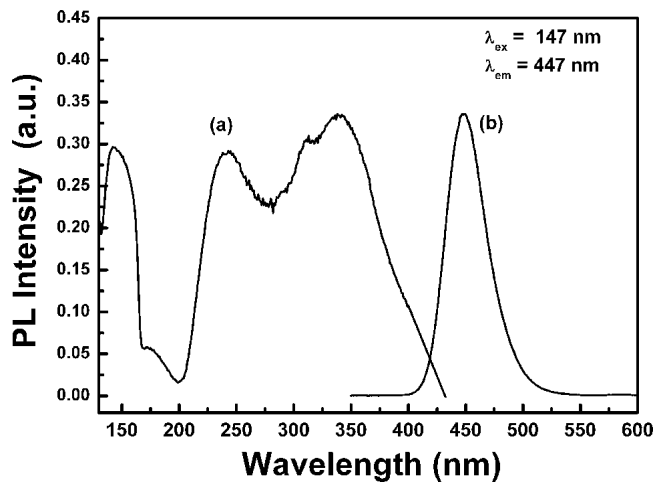


FIG. 5. (a) Excitation and (b) emission spectra of Ca_{0.99}MgSi_{2.2}O_{6.01}Eu²⁺ phosphor.

Taking the values of V , N , and X_c ($V = abc \sin\beta = 439.93 \text{ \AA}^3$, $N = 4$, $X_c = 0.01$, shown in Table I and Fig. 1), the critical transfer distance of Eu²⁺ in CMS:Eu²⁺ turned out to be 27 Å. From the calculated results mentioned above, the value of R_c is not well matched with the R_c obtained from the Dexter formula because the critical distance value using the critical concentration data involves the whole possible interaction between host lattice and activator. However, the critical distance value obtained using spectra overlap data considered dipole–dipole interaction.¹⁵ Furthermore, in the case of VUV excitation, the energy transfer process from the host lattice to the activator could play a significant role in PL process.^{1,16} Therefore, both reasons cause discrepancies in the critical distance values. Despite discrepancies in the critical distance values, we could expect that the critical distance value using the critical concentration data was more reasonable than the critical distance value obtained using spectra overlap data.

Nonradiative energy transfer from a Eu²⁺ ion to another Eu²⁺ ion may occur as a result of an exchange interaction, radiation reabsorption, or multipole–multipole interaction.^{12,13} Dexter¹² already reported that exchange interaction is responsible for energy transfer for forbidden transition and typical critical distance, which is about 5 Å. Because, in the case of CMS:Eu²⁺ phosphor, the energy transfer mechanism of Eu²⁺ is the $4f^7 \rightarrow 4f^65d$ allowed electric–dipole transition, the exchange interaction plays no role in energy transfer between Eu²⁺ ions. Therefore, the process of energy transfer will occur as an electric multipole–multipole interaction according to Dexter theory.¹² The emission intensity (I) per activator ion follows the equation given below^{17,18}

$$\frac{I}{C} = \frac{k}{[1 + \beta C^{\theta/3}]}, \quad (3)$$

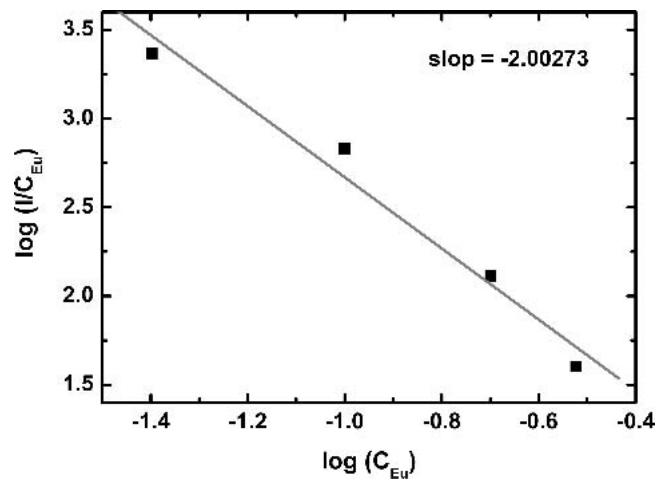


FIG. 6. Logarithm of the emission intensity per activator ion ($\log I/C_{\text{Eu}}$) as a function of logarithm of the Eu²⁺ concentration ($\log C_{\text{Eu}}$) in CMS:Eu²⁺ phosphor ($\lambda_{\text{ex}} = 147 \text{ nm}$).

where C is the activator concentration involved in self-concentration quenching, k and β are constants for each interaction in the same excitation conditions for a given host lattice. For $C \gg X_c$, the non-radiative losses are attributable to multipolar transfer, and for $\beta^{\theta/3} \gg 1$, Eq. (3) can be simplified as shown below

$$\frac{I}{C} = \frac{k_1}{\beta C^{\theta/3}}, \quad (4)$$

where k_1 is a constant.^{17,18} $\theta = 6, 8,$ and 10 are dipole–dipole, dipole–quadrupole, or quadrupole–quadrupole interactions, respectively. The value of θ can be determined from the slope ($-\theta/3$) of the linear line in Fig. 6, which plots $\log(I/C)$ versus $\log(C)$ on a logarithmic scale of I/C . The value of $-\theta/3$ is found to be -2.00273 . Therefore, the value of θ is calculated to be approximately 6. This indicates that the dipole–dipole interaction is the concentration quenching mechanism of Eu²⁺ emission in the CMS:Eu²⁺ phosphor.

IV. CONCLUSION

We optimized synthesis conditions of CMS:Eu²⁺ in terms of factors such as activator concentration, gas flow rates, and SiO₂ ratios, and successfully determined structure parameters by Rietveld refinement method with neutron powder diffraction data. In addition, we investigated fundamental luminescent properties of the optimized CMS:Eu²⁺. The concentration quenching process is observed, the critical quenching concentration of Eu²⁺ in CMS:Eu²⁺ is about 0.01 mol, and critical transfer distance of 12 Å is obtained. On the other hand, based upon the Rietveld refinement and Dexter theory, the critical transfer distance is calculated as 27 Å. Despite discrepancy in the critical distance values, we could expect

that the critical distance value using the critical concentration data was more reasonable than the critical distance value obtained using spectra overlap data. As a result of the fitting value between the emission intensity per activator concentration and activator concentration, the dipole–dipole interaction was a dominant energy transfer mechanism of electric multipolar character of CMS:Eu²⁺.

ACKNOWLEDGMENTS

This research was supported by a grant (M1-02-KR-01-0001-03-K18-01-025-1-3) from the Information Display R&D Center, part of the 21st Century Frontier R&D Program funded by the Ministry of Science and Technology of the Korean government.

REFERENCES

1. N. Youkosawa, G. Sato, and E. Nakazawa: Improvement of luminescence degradation of PDP blue phosphor with new UV phosphor. *J. Electrochem. Soc.* **150**, H197 (2003).
2. T. Kunimoto, R. Yoshimatsu, K. Ohmi, S. Tanaka, and H. Kobayashi: Feasibility study of silicate phosphor CaMgSi₂O₆:Eu²⁺ as blue PDP phosphor. *IEICE Trans. Electron.* **E85-C**, 11 (2002).
3. W.B. Im, J.H. Kang, D.C. Lee, S. Lee, D.Y. Jeon, Y.C. Kang, and K.Y. Jung: Origin of PL intensity increase of CaMgSi₂O₆:Eu²⁺ phosphor after baking process for PDPs application. *Solid State Commun.* **133**, 197 (2005).
4. A.C. Larson and R.B. Von Dreele: General Structure Analysis System (GSAS). *Los Alamos National Laboratory Report LAUR.* **86**, 748 (1994).
5. R.C. Ropp: *Luminescence and the Solid State* (Elsevier, the Netherlands, 1991), Chap. 8.
6. *Phosphor Handbook*, edited by S. Shinoya and W.M. Yen (CRC Press, 1998), Chap. 5.
7. L.W. Finger, D.E. Cox, and A.P. Jephcoat: A correction for powder diffraction peak asymmetry due to axial divergence. *J. Appl. Crystallogr.* **27**, 892 (1994).
8. L. Levien and C.T. Prewitt: High-pressure structural study of diopside. *Am. Mineral.* **66**, 315 (1981).
9. N.R. Keskar and J.R. Chelikowsky: Structural properties of nine silica polymorphs. *Phys. Rev. B* **46**, 1 (1992).
10. R.D. Shannon: Revised effective ionic radii and systematic studies of interatomic distances in halides and chalcogenides. *Acta Crystallogr. A* **32**, 751 (1976).
11. G. Blasse and B.C. Grabmaier: *Luminescent Materials* (Springer-Verlag, Germany, 1994), Chap. 3.
12. D.L. Dexter: A theory of sensitized luminescence in solids. *J. Chem. Phys.* **21**, 836 (1953).
13. G. Blasse: Energy transfer in oxidic phosphors. *Philips Res. Repts.* **24**, 131 (1969).
14. G. Blasse: Energy transfer between inequivalent Eu²⁺ ions. *J. Solid State Chem.* **62**, 207 (1986).
15. S.H. Shin, D.Y. Jeon, and K.S. Suh: Charge-transfer nature in luminescence of YNbO₄:Bi blue phosphor. *J. Appl. Phys.* **90**, 12 (2001).
16. K.S. Sohn, B.H. Cho, and H.D. Park: Excitation energy-dependent photoluminescence behavior Zn₂SiO₄:Mn phosphors. *Mater. Lett.* **41**, 303 (1999).
17. L.G. Van Uitert: Characterization of energy transfer interactions between rare earth ions. *J. Electrochem. Soc.* **114**, 1048 (1967).
18. L. Ozawa: *Cathodoluminescence: Theory and Applications* (VCH, Japan, 1990), Chap. 6.